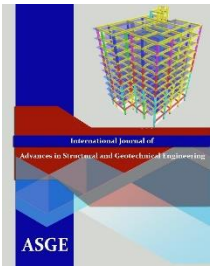

International Journal of Advances in Structural and Geotechnical Engineering

https://asge.journals.ekb.eg/

Print ISSN 2785-9509 *Online ISSN 2812-5142*

Special Issue for ICASGE'19

Experimental and Numerical Investigations on the Flexural Behavior of RC Castellated Beams

Abdelaziz Nabil, Hamdy M. Afefy, Nesreen M. Kassem, and Salah El-Din F. Taher

ASGE Vol. 04 (02), pp. 44-61, 2020

International Conference on Advances in Structural and Geotechnical Engineering

ICASGE'19

25-28 March 2019, Hurghada, Egypt

Experimental and Numerical Investigations on the Flexural Behavior of RC Castellated Beams

Abdelaziz Nabil [1], Hamdy M. Afefy[2], Nesreen M. Kassem[3], Salah El-Din F. Taher[4]

[1]Demonstrator, Faculty of Engineering, Tanta University, Egypt
E-mail: Abdelaziz_nabil@f-eng.tanta.edu.eg
[2] Professor, Faculty of Engineering, Tanta University, Egypt
E-mail: hamdy.afefy@f-eng.tanta.edu.eg
[3]Associate Professor, Faculty of Engineering, Tanta University, Egypt
E-mail: nesreen.kassem@f-eng.tanta.edu.eg
[4]Professor, Faculty of Engineering, Delta University for Science and Technology.
On leave from Tanta University, Egypt
E-mail: salah.taher@f-eng.tanta.edu.eg

ABSTRACT

This paper presents both experimental and numerical studies on the flexural performance of reinforced concrete beams having hexagonal (castellated) web openings. At first, a parametric study using ABAQUS program has been conducted on the governing parameters of the castellated beams. The studied parameters were the percentage of longitudinal main steel, the configuration of the reinforcing steel around the castellation, and the effect of providing side reinforcement above and below the castellation. Based on the results of the parametric study, the best configuration of the reinforcing steel around the castellation was selected based on the manifested flexural behavior. Thus, the test specimens to be tested experimentally were configured. One solid beam and another castellated beam have been tested under the effect of incremental concentrated load at the mid-span point. The obtained responses along with the mode of failure from the experimental test are compared with the predicted ones from the numerical simulation. Comparison shows good agreement between the displayed mode of failure, ultimate capacity and the developed mid-span deflection obtained from both numerical simulation and the experimental tests.

Keywords: ABAQUS software, Finite Element Method, Beam with hexagonal openings, Castellated beam.

INTRODUCTION

These days, providing web openings in reinforced concrete beams in modern reinforced concrete structures became a common practice [1].Openings in general are areas of weakness and stress concentration needed essentially for passing ducts and piping for different service facilities such as air conditioning, sewages water supply and computer networks. They can take any shape such as circular, rectangular, square, hexagonal and oval; however the circular and the rectangular configurations are the most common shapes [2, 3]. With regard to the size of openings, many researchers use the terms ‘‘small’’ and ‘‘large’’ without drawing any clear-cut demarcation line. The classification as small or large opening is based on either the size of opening and/or the overall structural performance of the beam containing this opening. Mansur et al. [4] and Hasnat and Akhtaruzzaman [5] classified all circular and nearly square openings as small openings. However, Somes and Corley [6] classified the circular opening of diameter less than 0.25 times the total depth of the beam as small one; otherwise the opening may be classified as large opening. Mansur and Tan [7] classified the small opening as that the opening whose diameter is less than 0.40 times the total depth of the beam, otherwise, the opening may be considered as large one. Aykac and Yilmaz [8] found that circular openings are more efficient than triangular

openings from the ductility viewpoint. Furthermore, it was found that introducing large opening without providing proper internal reinforcement could reduce the ultimate capacity significantly [9]. However, providing sufficient diagonal reinforcement around the openings eliminated shear failure of the web posts and prevented premature failure of the beam [10].

In the current study, a new perforated beam system is developed and tested. Numerical analysis using ABAQUS software [11] was used in order to verify the effect of providing castellation on the beam performance as well as to assist in choosing the reinforcement configuration of the castellated beam to be tested experimentally. The effect of the area of main steel, the effect of area of side steel, the configurations of the provided internal reinforcement around the perforations were the main studied parameters. Based on the results of the numerical parametric study, refined parameters were implemented on one castellated beam. In addition, another solid beam was considered as a reference control one. Finally, the results of the experimental tests were compared with the numerical findings to verify the numerical simulation of the castellated beam.

FINITE ELEMENT MODELING

In this part, the adopted failure criteria of both concrete and reinforcing steel bars were explained along with their behavior in tension and compression. Besides, the elements representation was outlined for both concrete and reinforcing steel. Finally, a verification of the modeling parameters was conducted by comparing the resulting response of already tested beam with the results of the numerical simulation for that beam considering the adopted parameters.

In this paper concrete damage plasticity model was chosen to model the concrete behavior. This model assumes that the main two failure modes are tensile cracking and compressive crushing as will be illustrated here in below.

Uniaxial tension behavior of concrete

Concrete behaves linearly elastic in the first stage of its tensile behavior. In this stage the tensile stress , $f_{ct,}$ is linearly proportionate the tensile strain through elastic modulus, E_c, [12] as shown in Fig.1.

$$E_c = 4400\sqrt{f_{cu}} \quad \text{(MPa)} \qquad (1)$$

$$f_{ct} = 0.6\sqrt{f_{cu}} \quad \text{(MPa)} \qquad (2)$$

Where f_{cu} = concrete compressive cubic strength.

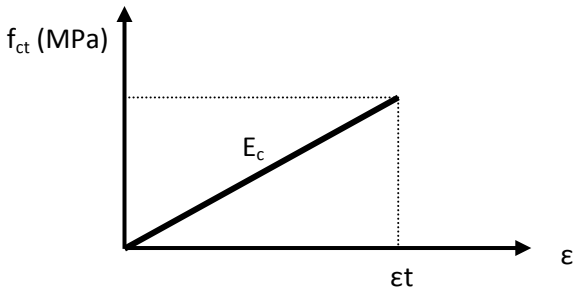

Fig.1. Stress-strain relationship under uni-axial tension up to first cracking load.

In the second stage; tension softening starts where micro cracks grow to macro cracks and stiffness significantly decreases to zero. Concrete damage plasticity model in ABAQUS tension softening is defined by stress-strain or stress-displacement relationships and to specify the post-peak tension failure behavior of concrete, the fracture energy method was used. The fracture energy can be estimated by the following equation proposed by Hillerborg [13] as depicted in Fig.2:

$$G_f = 110\left(\frac{f_{cy}}{10}\right)^{0.18} \quad \text{Jole/m}^2 \qquad (3)$$

Where Gf = fracture energy; f_{cy} = concrete cylindrical compressive strength

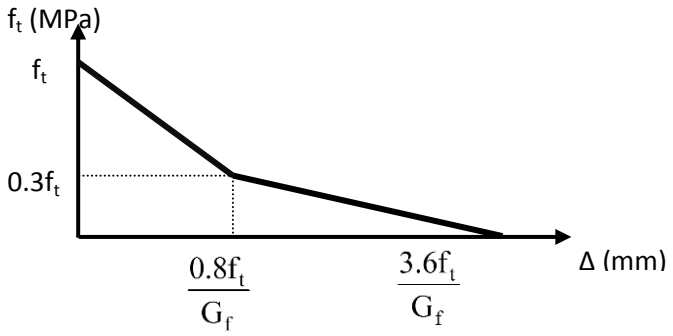

Fig.2. Post-peak stress deformation relationship under uniaxial tension.

Uniaxial compressive behaviour of concrete

For the compression stress-strain curve of the concrete, the stress–strain relationship proposed by Park and Paulay [14] was used to construct the uni-axial compressive stress–strain curve for concrete as shown in Fig.3. Poisson's ratio was assumed to be 0.22

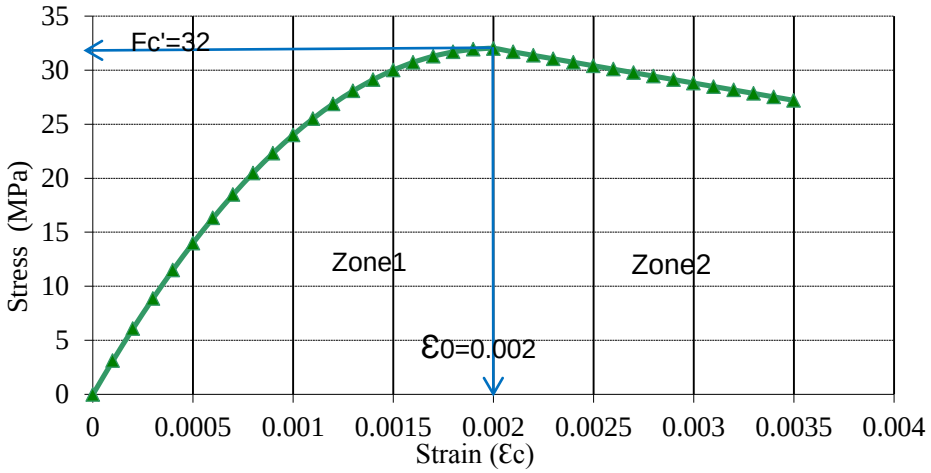

Fig.3. Schematic diagram of adopted concrete stress-strain behavior in compression.

$$\text{when} \quad \varepsilon \le 0.002, \qquad f_c = f_c' \left[2\frac{\varepsilon_c}{\varepsilon_0} - \left(\frac{\varepsilon_c}{\varepsilon_0} \right)^2 \right] \qquad (4)$$

$$\text{when} \quad 0.002 \le \varepsilon \le 0.0035, \qquad f_c = f_c' \left[1 - 0.15\frac{\varepsilon - \varepsilon_0}{\varepsilon_{cu} - \varepsilon_0} \right] \qquad (5)$$

Steel reinforcement

The behavior of reinforcing steel bars was assumed to be bilinear elasto–plastic material and identical in tension and compression as depicted in Fig.4. Elastic behavior of steel material is defined by specifying Young's modulus (E_s) and Poisson's ratio (v) of which typical values are 2 x 10^5 MPa and 0.3, respectively. The bond between steel reinforcement and concrete was assumed to be perfect bond.

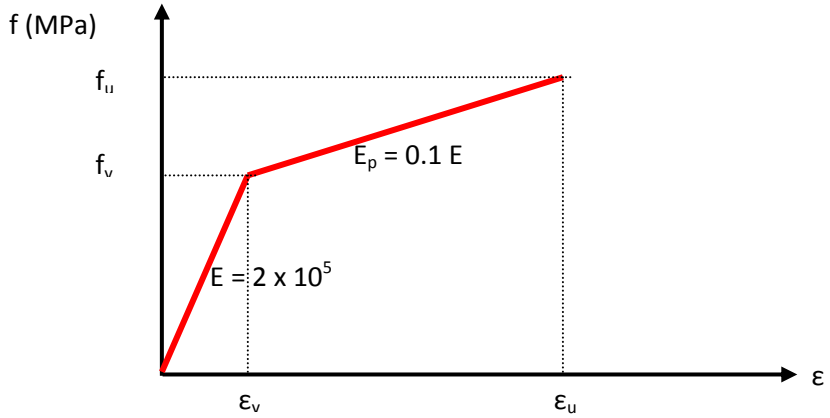

Fig.4. Idealized stress-strain curve for steel reinforcement.

Finite element mesh

In order to obtain accurate results from the FE model, all the elements in the model were assigned the same mesh size to ensure that each two different materials share the same nodes. The selected mesh element for concrete is 3D solid which is called C3D8R and for the rebar is 2D truss which is called T3D2.

Verification of finite element program

To verify the model of finite element program for reinforced concrete beams, control beam tested by Atta and Khalil [15] has been chosen. The beam had length 3200mm with cross-section of 150 x 400 mm. The beam was reinforced with four lower bars of 16 mm diameter and two upper bars of 12 mm diameter. Smooth bars of 8 mm diameter were used for stirrups arranged at different spacing along the beam length as shown in Fig.5. The average cube compressive strength was 30 MPa. The longitudinal reinforcement used in the specimens was high tensile steel reinforcement with average yield and ultimate strengths of 450 MPa and 610 MPa, respectively. For web reinforcement, ordinary reinforcement with average yield strength of 250 MPa was used. A comparison of load deflection curves from test and analysis showed that the finite element program explicated the structural behavior of the beam satisfactorily as depicted in Fig.6.

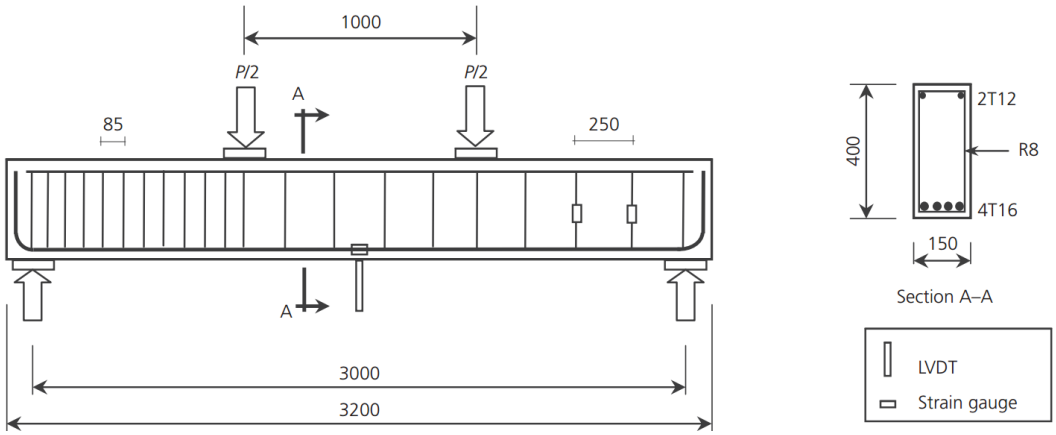

Fig.5. Dimensions and reinforcement details of tested beam by Atta and Khalil (2015) used for verification of the numerical simulation.

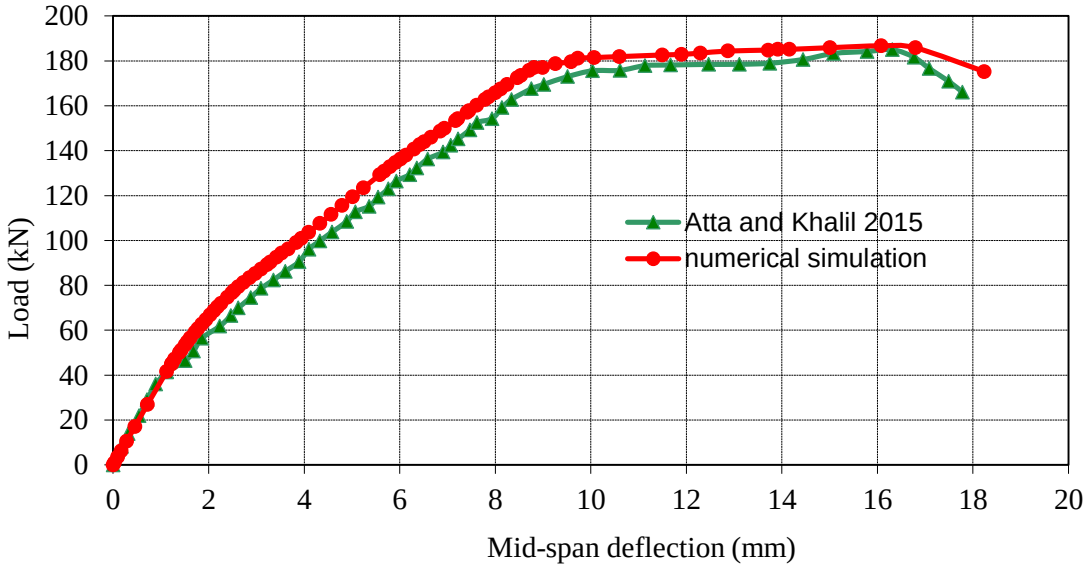

Fig.6. Comparison between the experimental and the finite element results.

PARAMETRIC STUDY

Material properties

For the current parametric study, the average cube compressive strength of the used concrete was 40 MPa. While, the used longitudinal reinforcing steel bars was deformed high tensile steel with average yield and ultimate strengths of 400 MPa and 600 MPa, respectively. For web reinforcement, ordinary smooth bars with average yield and ultimate strengths of 280 MPa and 450 MPa, respectively was used.

Effect of the percentage of longitudinal main steel

In order to study the effect of different ratios of longitudinal reinforcement, four concrete beams with 4 ratios have been modeled. The beams had total length of 2500mm, while center-to-center span was 2300mm and cross-section was120 x 400 mm. The beams were reinforced with two lower bars of different diameters (12-16-18-22) mm and with two upper longitudinal bars of 10 mm diameter. Smooth bars of 8 mm diameter were used for stirrups that were provided at 100 mm spacing along the beam length as shown in Fig.7.

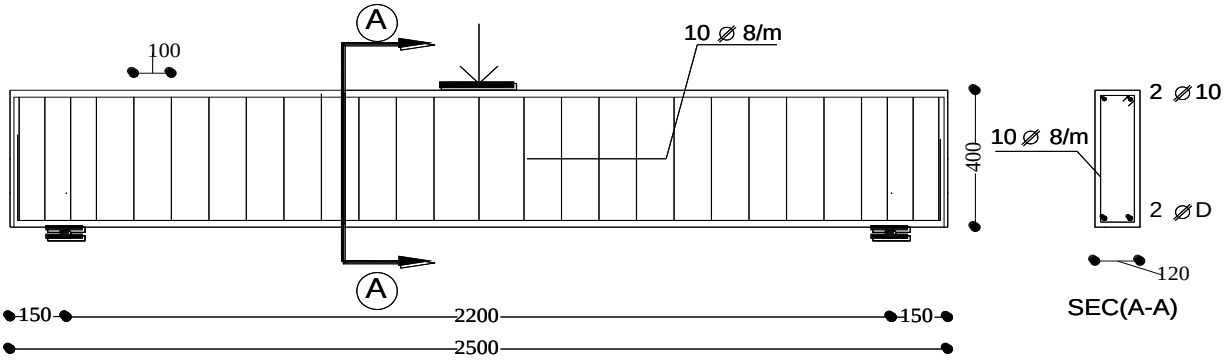

Fig.7. Dimensions and reinforcement details of tested beams.

All beams were tested under the effect of incremental concentrated load applied at the mid-span point. Thus, the maximum bending moment will be induced at the mid-span point and decreases linearly till zero value at the supporting points, while the developed shearing force will be constant along the entire beam.

All beams were loaded till complete failure which was flexural mode for all beams as depicted in Fig. 8. For all beams, the mid-span deflection versus the acting load relationship was plotted and compared as shown in Fig. 9. Besides, the displacement-based ductility index was calculated for each beam based on the load-deflection relationship and compared with the reaming beams.

It was noticed that increasing the amount of the main steel has shown obvious effect on both ultimate capacity and ductility. The ultimate capacity of beam was noticed to be directly proportionate to the amount of the main longitudinal steel. On the other hand, the developed ductility was inversely proportionate with the amount of main steel as listed in Table1. Therefore, we decided to use the main steel in experimental work as two bars of 16mm diameter in order to obtain acceptable ultimate capacity and ductility. Besides, the overall concrete dimensions, compression steel and stirrups are kept constant for the others beams considering the remaining parameters.

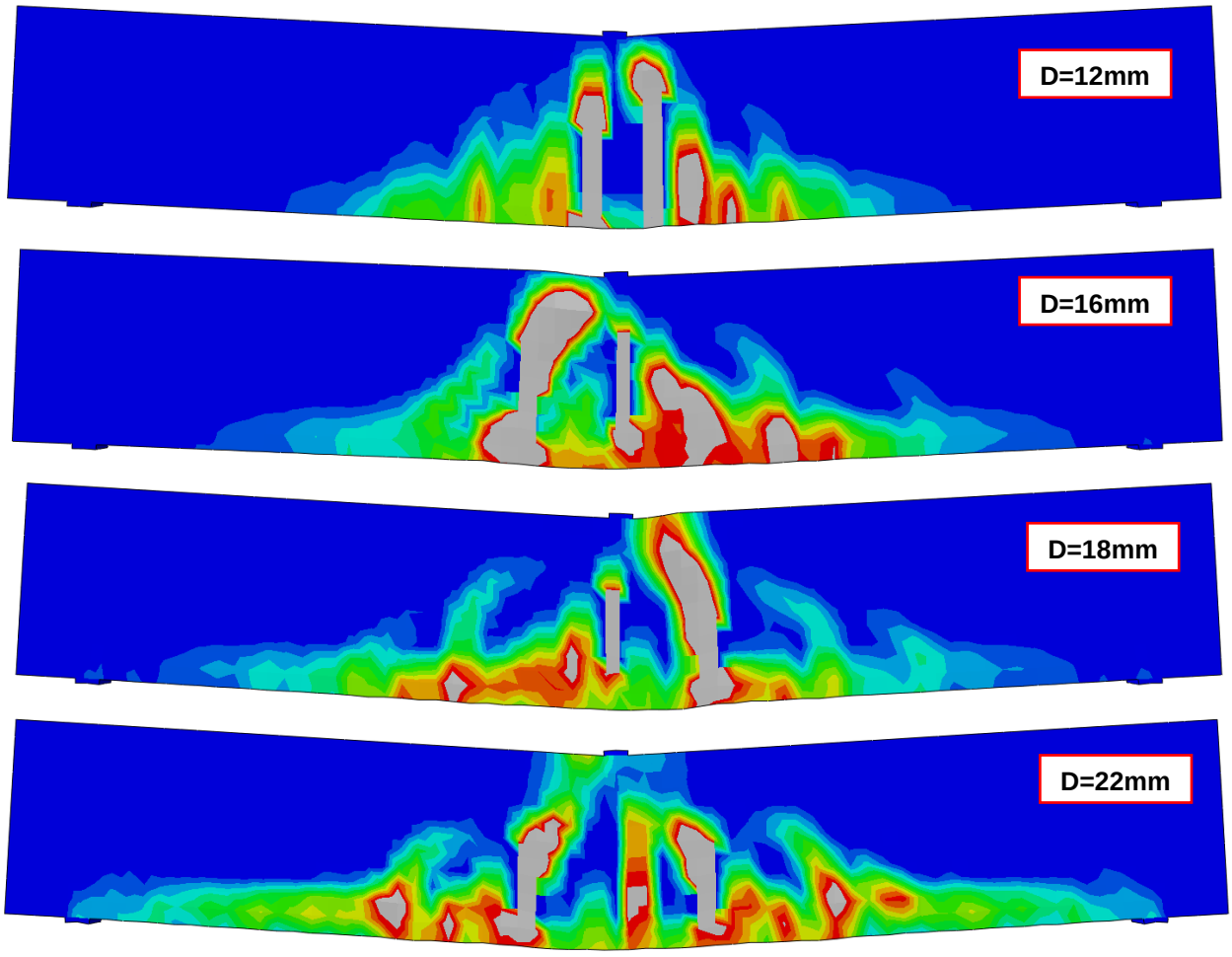

Fig.8. Modes of failure of beams with different longitudinal main steel diameter.

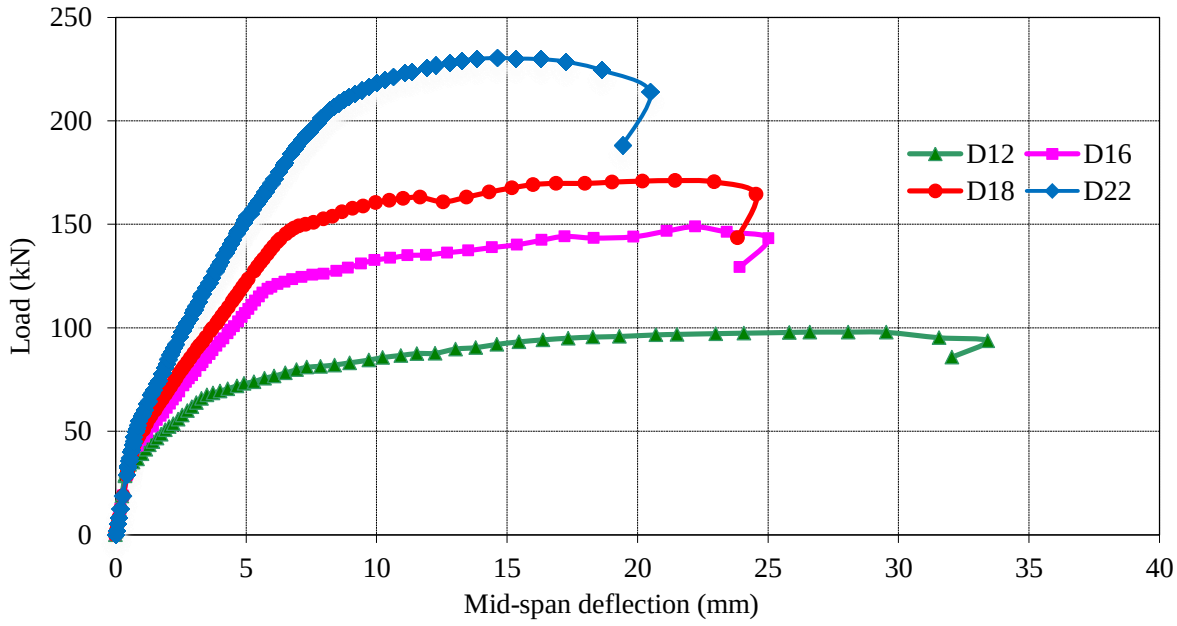

Fig.9. Load-deflection relationships for beams taking into account different diameters for the main reinforcing steel.

Table 1 Ultimate capacities and developed ductility indices corresponding to variation of the diameter of main reinforcing steel

Diameter of main steel (mm)	ultimate capacity(KN)	$\Delta ultimate$ (mm)	$\Delta yield$ (mm)	$Ductility\ index = \frac{\Delta_{ultimate}}{\Delta_{yield}}$
12	97.7	28	3.3	8.48
16	148.8	22.2	5.6	3.96
18	183.8	21.4	6.5	3.29
22	293.5	15.3	7.8	1.96

Effect of reinforcement configuration around the castellation

Previous studies [16] showed that the reinforcement configuration around the openings has significant effect on both the ultimate capacity and the developed ductility of RC beams having web openings. For the current study, three concrete beams with castellated opening (D/t=0.48) and different shapes of reinforcing steel around the castellation have been modeled as depicted in Fig. 10. The beams had total length of 2500mm and cross-section 120 x 400 mm. The beam was reinforced with two lower bars of 16 mm, and with two upper bars of 10 mm diameter. It was found that the castellated beam adopted shape 1 developed the best performance among the considered shapes from the view point of ultimate capacity, failure pattern and the exhibited ductility as illustrated in Figs. 11 and 12 as well as Table 2. Thus, this shape of reinforcement was considered in the upcoming parametric study as well as the experimental program.

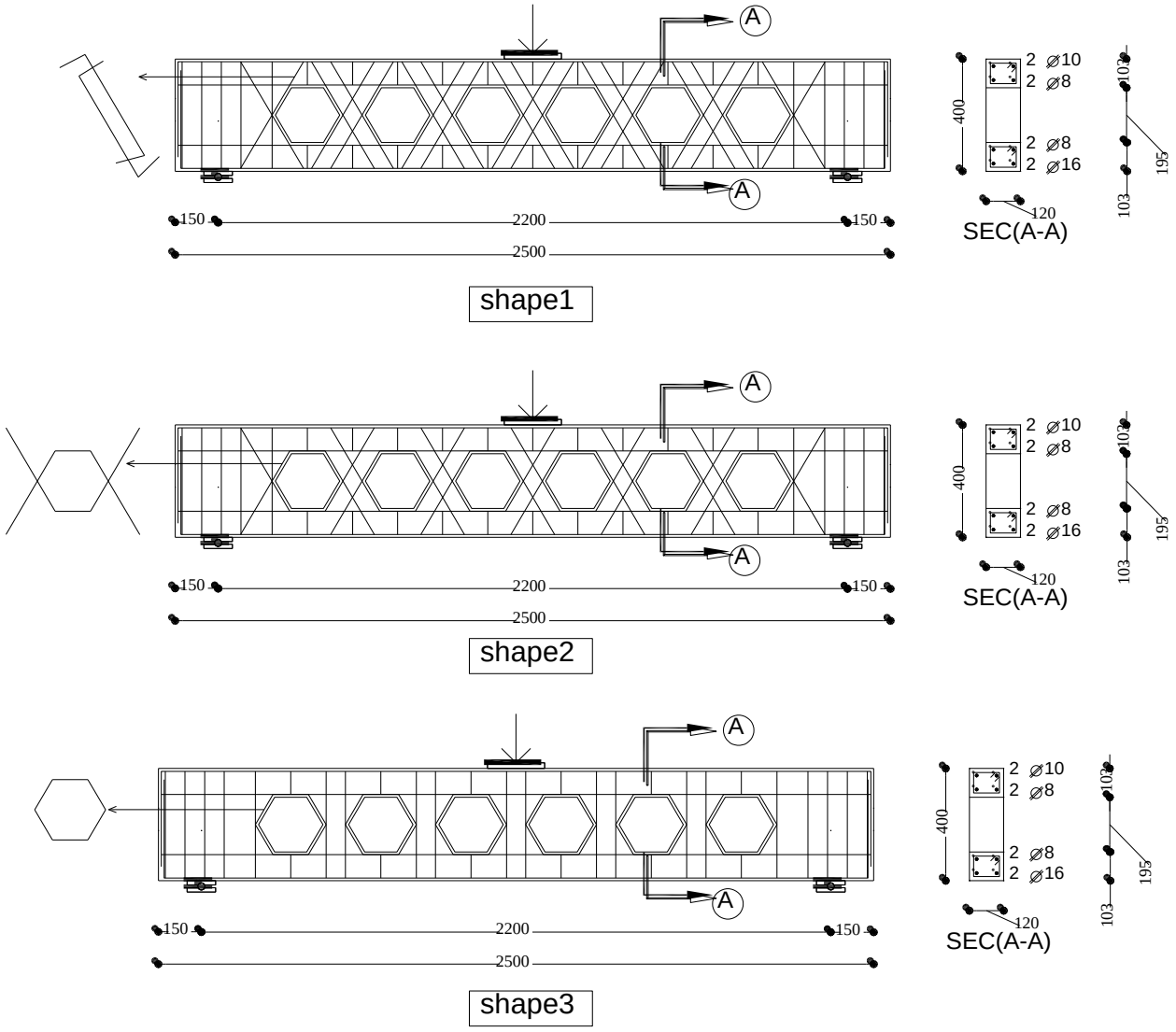

Fig.10. Dimensions and different reinforcement details around the castellation.

Table 2 Ultimate capacities and developed ductility indices corresponding to different configurations of reinforcing steel around the castellation

Shape of steel around the castellation	ultimate capacity(KN)	$\Delta ultimate$ (mm)	$\Delta yield$ (mm)	$Ductility\ index = \frac{\Delta_{ultimate}}{\Delta_{yield}}$
Shape1	154.3	21.3	6.5	3.27
Shape2	111.8	8.5	5.3	1.6
Shape3	88.6	4.8	3.1	1.55

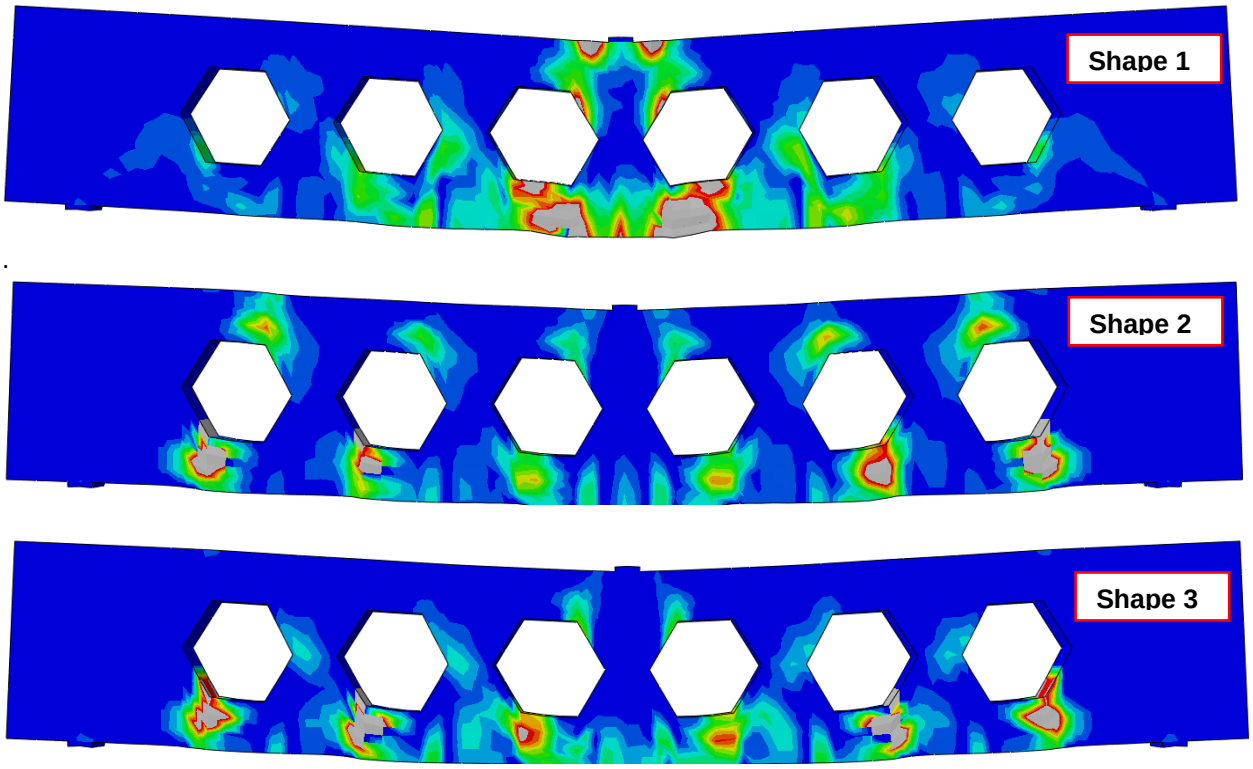

Fig.11. Modes of failure of beams with different configurations of reinforcing steel around the castellation.

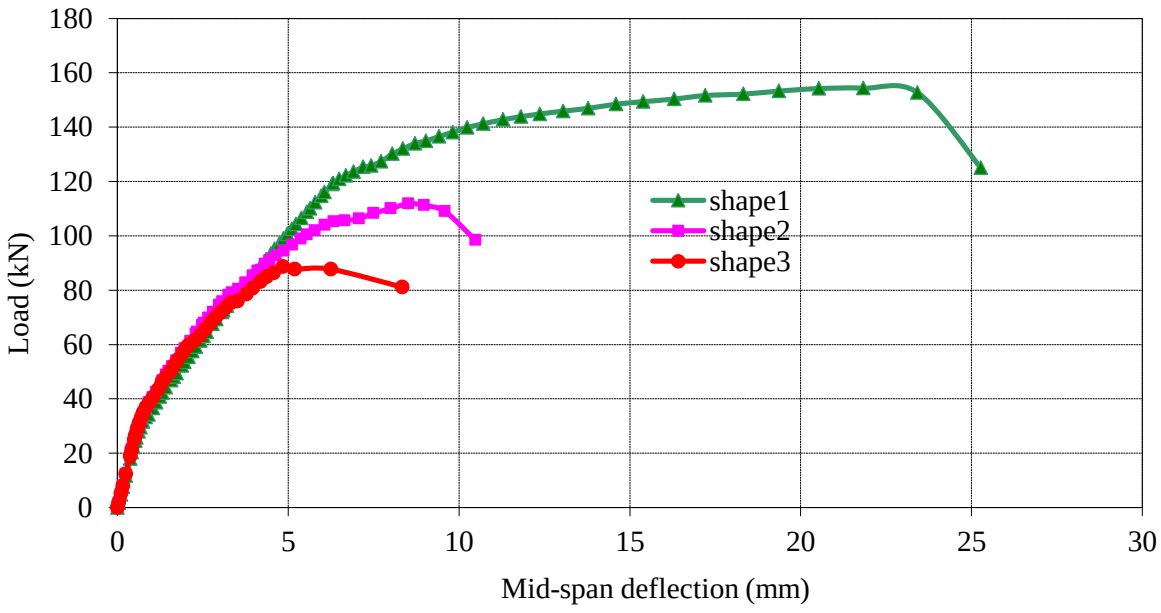

Fig.12. Load-deflection relationships corresponding to different configuration of reinforcing steel around the castellation.

Effect of providing side reinforcement above and below the castellation

For this comparison, three beams were considered; castellated beam having reinforcement shape 1, solid beam without side reinforcement and solid beam provided with side reinforcement as depicted in Fig. 13. Numerical simulation of the three beams till complete failure revealed that the ultimate capacity of castellated beam was higher than that of solid beam without side reinforcement by about 3.5%. However, providing side reinforcement for the solid beam enabled it to outperform the ultimate capacity of the castellated beam by about 6% (refer to Fig. 14). In addition, providing side reinforcement in solid beam resulted in increased both ultimate capacity and ductility of solid beam significantly as illustrated in Table 3.

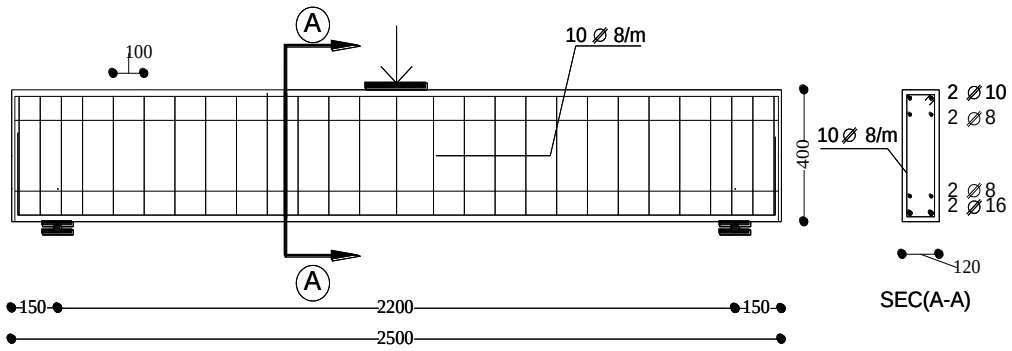

Fig.13. Dimensions and reinforcement details of solid beam with side reinforcement.

Table 3 Ultimate capacities and developed ductility indices taking into account the effect of side reinforcement above and below the castellation

Beam name	ultimate capacity(kN)	$\Delta ultimate$ (mm)	$\Delta yield$ (mm)	$Ductility\ index = \frac{\Delta_{ultimate}}{\Delta_{yield}}$
Castellated	154.3	21.3	6.5	3.27
Solid without sides reinforcement	148.8	22.2	5.6	3.96
Solid with sides reinforcement	163.1	24.6	5.6	4.39

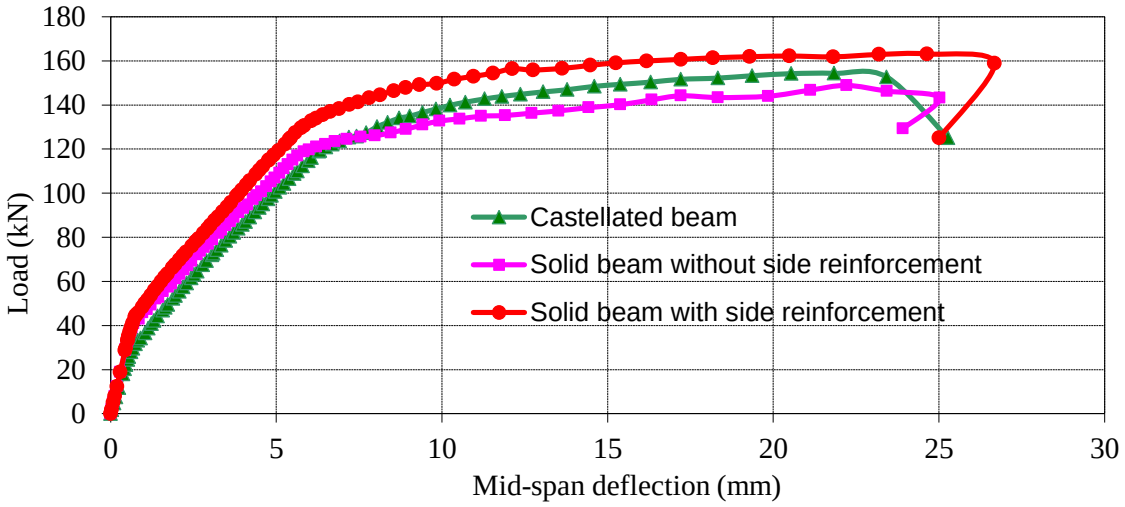

Fig.14. Load-deflection relationships considering the effect of side reinforcement.

In order to study the effect of providing side reinforcement above and below the castellation, solid and castellated beams were considered. The beams were reinforced with two lower bars of 16 mm diameter, and with two upper bars of 10 mm diameter. Side bars had different diameters (8-10-12) mm.
For solid beam with increasing diameter of side bars the ultimate capacity of beam increases while ductility of beam decreases as depicted in Fig. 15. On the other hand, the size of the diameter of side bars in castellated beam affects slightly the ultimate capacity and ductility as shown in Fig. 16. Therefore, it was decided to use side bars with 8 mm diameter in the experimental program.

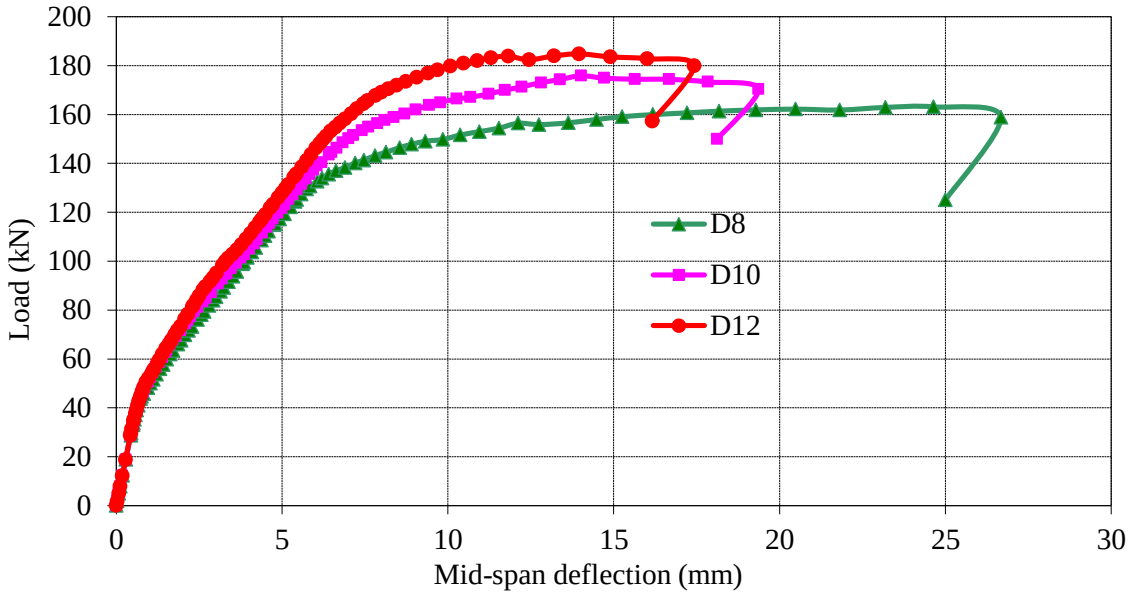

Fig.15. Load-deflection curves for solid beam with different side bars diameter.

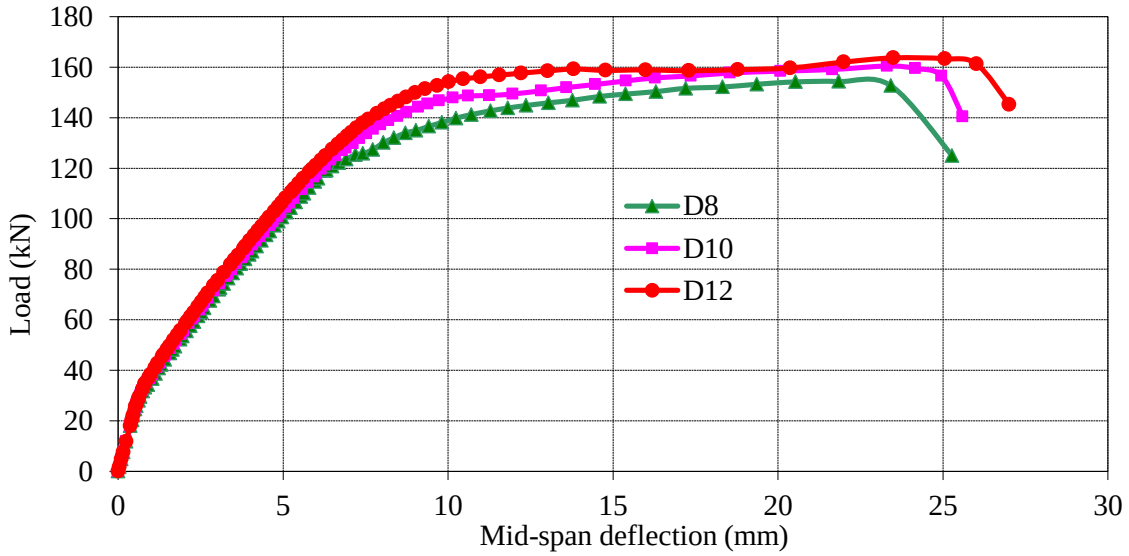

Fig.16. Load-deflection relationships for castellated beam with different side bars diameter.

EXPERIMENTAL WORK PROGRAM

Test specimens

The experimental program consists of two simple beams; one solid beam and another castellated beam. Beams had cross section of 120 x 400 mm, and a total length of 2500 mm, while the center-to-center span was 2200 mm. The beams were reinforced with two lower bars of 16 mm diameter, and with two upper bars of 10 mm diameter. R8 bars were provided for web reinforcement. Castellated beam had perforation height of 195 mm (D/t=0.48) with the best shape of reinforcing steel around the castellation based on the numerical investigation as depicted in Fig. 17.

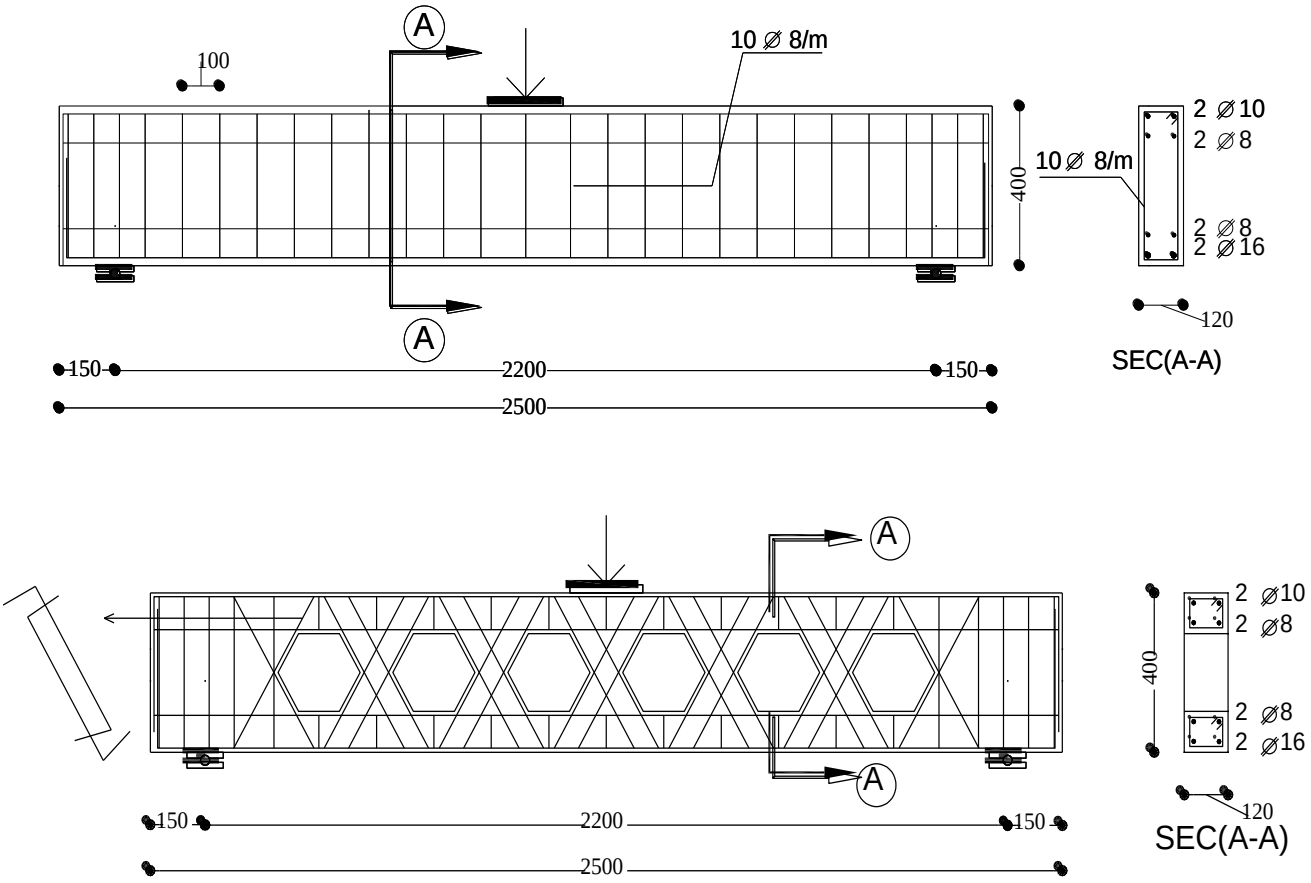

Fig.17. Dimensions and reinforcement details of tested beams.

Manufacturing of specimens

The following images of Fig. 18 illustrate step by step the preparation procedure for both solid and castellated beams considering the formwork assembly, reinforcing steel cages and casting the beams.

Fig.18-a. Wooden form.

Fig.18-b. Reinforcing steel cage for solid and castellated beams.

Fig.18-c. Solid and castellated beams just before casting.

Fig.18-d. Solid and castellated beams after concrete casting.

Fig. 18 Preparation and casting of solid and castellated beams.

Material properties

The used concrete was a ready-mix concrete of target concrete compressive strength of 40 MPa. The actual compressive strength was calculated as the average value of three pre-prepared standard cubes of 150 mm side length that were collected from different locations at the casting day. The average compressive strength was about 41.1MPa. The tensile strength was calculated using Brazilian Tensile Test with as the average value of three pre-prepared standard cylinder of 300 x150 mm. The average tensile strength of concrete was about 3.02 MPa. For the longitudinal steel bars as well as the stirrups, in order to determine the mechanical properties, tensile tests were performed on three specimens for each bar size. Table 4 summarizes the mean values of tensile yield strength, ultimate strength and Young's modulus for each bar size.

Table 4 Mechanical properties of the used steel bars.

Bar diameter, mm	Type	Average yield strength, MPa	Average tensile strength, MPa	Average modulus of elasticity, GPa
16	Deformed	410	623	204
10	Deformed	415	604	202
8	Smooth	283	456	199

Test setup

The experimental program has been carried out at the reinforced concrete laboratory of the Faculty of Engineering, Tanta University, Egypt. In order to measure the deformed shapes of all beams, three LVDTs having 100 mm gauge length were used as shown in Fig. 19. The developed normal strains on the tensile steel bars were measure by strain gauges of 10 mm gauge length. In addition, the developed strains on the concrete surface were measured by 100 mm Pi-gauges. The specimen ends were simply-supported over roller support at one end and hinged support at the other end. Beams were loaded by one concentrated load in the mid-span point. The beams were loaded incrementally under static loading up to complete collapse. The load on the beams was measured by a load cell of 600 kN capacity. After each loading step, the vertical deflections along the measuring points, the developed normal strains in the steel bars as well as the developed strains on the concrete surface were recorded and stored by an automatic data logger unit (TDS-150).

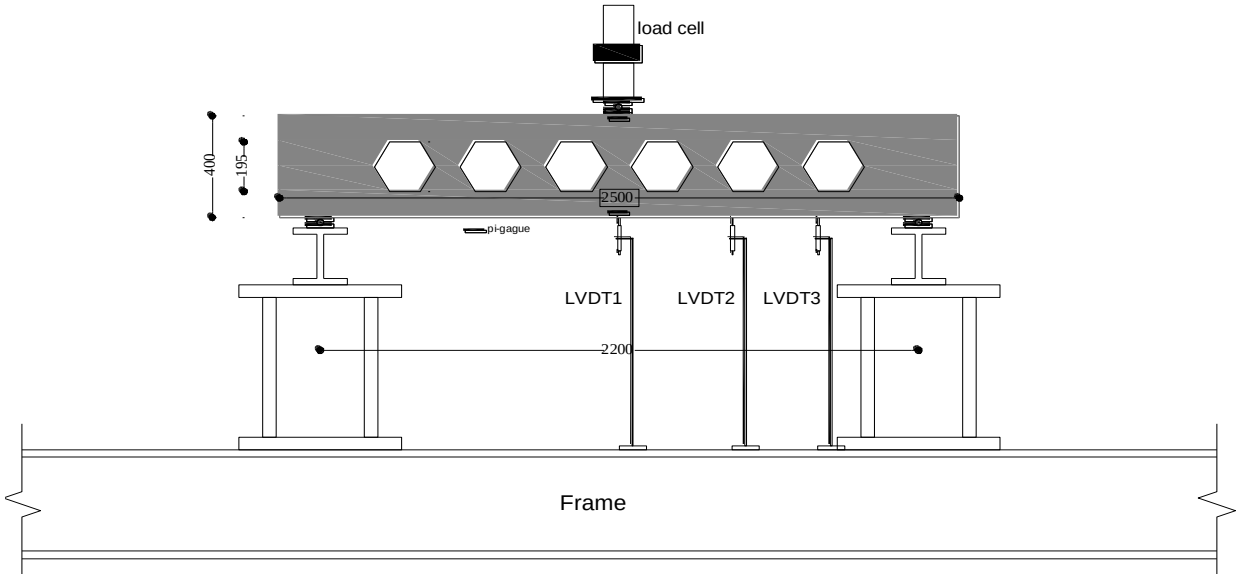

Fig.19. Test setup.

Comparison between numerical and experimental results

In order to investigate the efficiency of numerical simulation, a comparison between numerical load-deflection responses was compared with that measured during testing of both beams. Comparison showed good agreement between the ultimate capacity and the developed mid-span deflection obtained from both numerical simulation and the experimental tests as depicted in Figs 20 and 21.

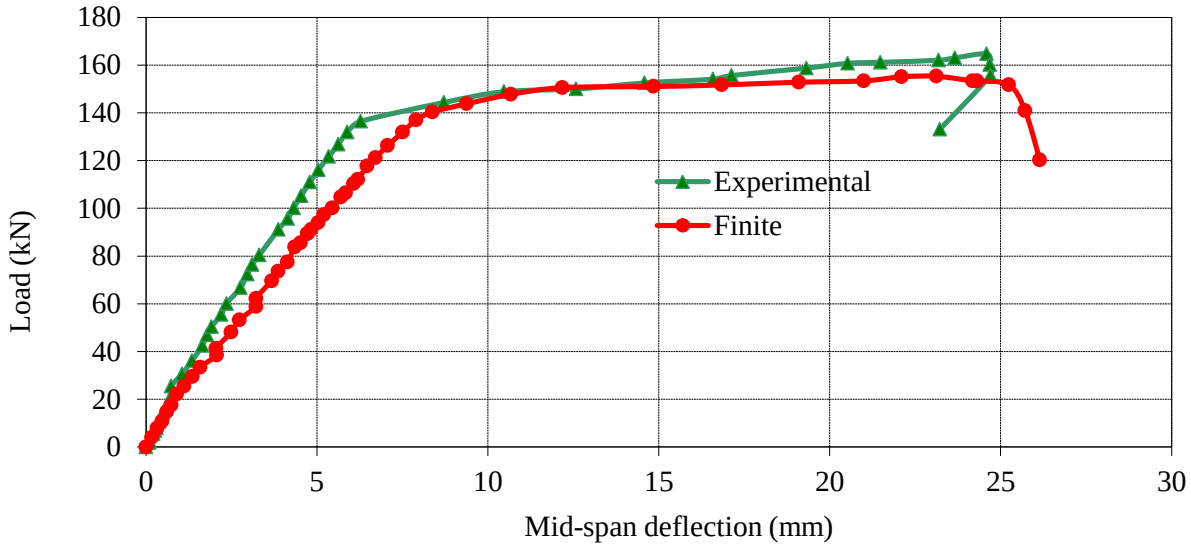

Fig.20. Comparison between experimental and numerical results of the load-deflection response for solid beam.

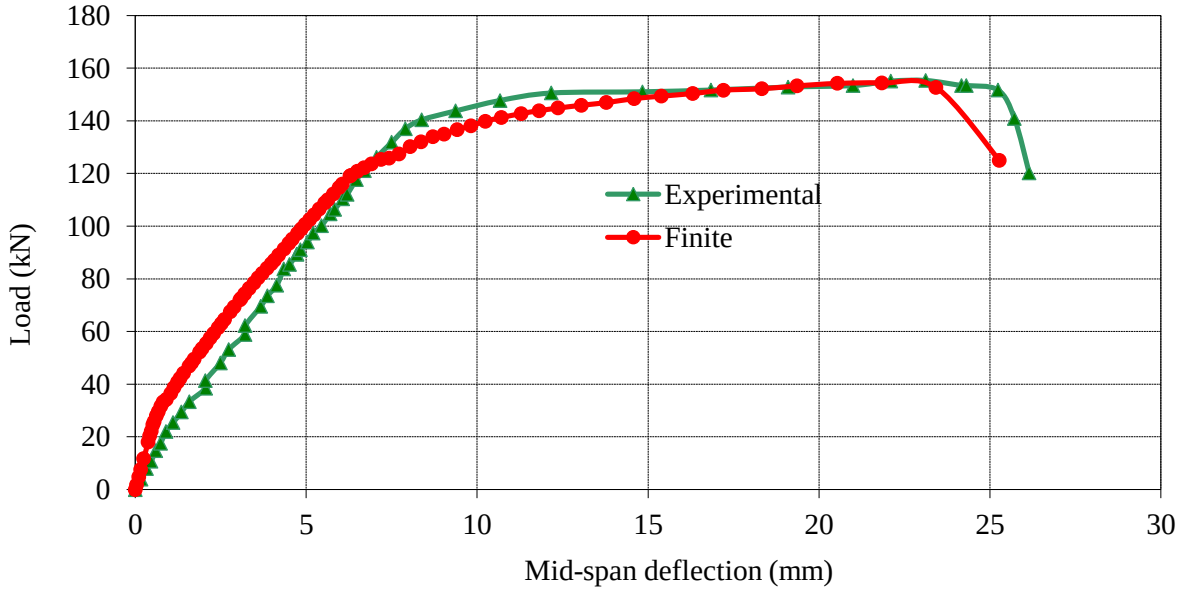

Fig.21. Comparison between experimental and numerical results of the load-deflection response for castellated beam.

Experimental results and discussion

Table 5 summarizes the experiment results of both solid and castellated beam.

Table 5 Experimental results for solid and castellated beams

Criteria	Solid beam	Castellated beam
First flexural cracking load, kN	35	29
First shear cracking load, kN	132	103
The ultimate load, kN	164.7	155.3
$\Delta ultimate$ (mm)	24.6	23.1
$\Delta yield$ (mm)	6.0	7.8
$Ductility\ index = \frac{\Delta_{ultimate}}{\Delta_{yield}}$	4.1	2.96

For solid beam, the first flexural crack started to appear at the mid-span section of the beam at a vertical load of about 35 kN. Proceeding with loading, the flexural cracks spread at the tension side till a vertical load of about 132 kN, and then shear cracks began to appear. Soon later the beam was no longer sustained more loading and the crack width of the major flexural crack exceeded 1.0 mm and the beam reached complete failure at a vertical load of about 164.7 kN as depicted in Fig. 22.

Castellated beam started to develop crack due to flexure at the mid span section at a vertical load of about 29 kN, while, the first cracking due to shear started to appear at a vertical load of about 103 KN. With further loading, the flexural cracks spread at the tension side till a sudden local shear crack appeared in the upper chord and the beam reached failure at a vertical load of 155.3 KN illustrated in Fig. 23.

It can be observed that providing castellation in RC beams accelerated the appearance of cracks due to both flexure and shear stresses compare to those of the solid beam. In addition, providing castellated perforations in reinforced concrete beam has shown slight decrease in the ultimate load carrying capacity by about 5.3 % compared with solid beam and significant decrease in the exhibited ductility by about 27.8 % compared with that of solid beam. In addition, castellated beam showed decrease stiffness up to approaching failure load compared with the solid beam.as shown in Fig. 24.

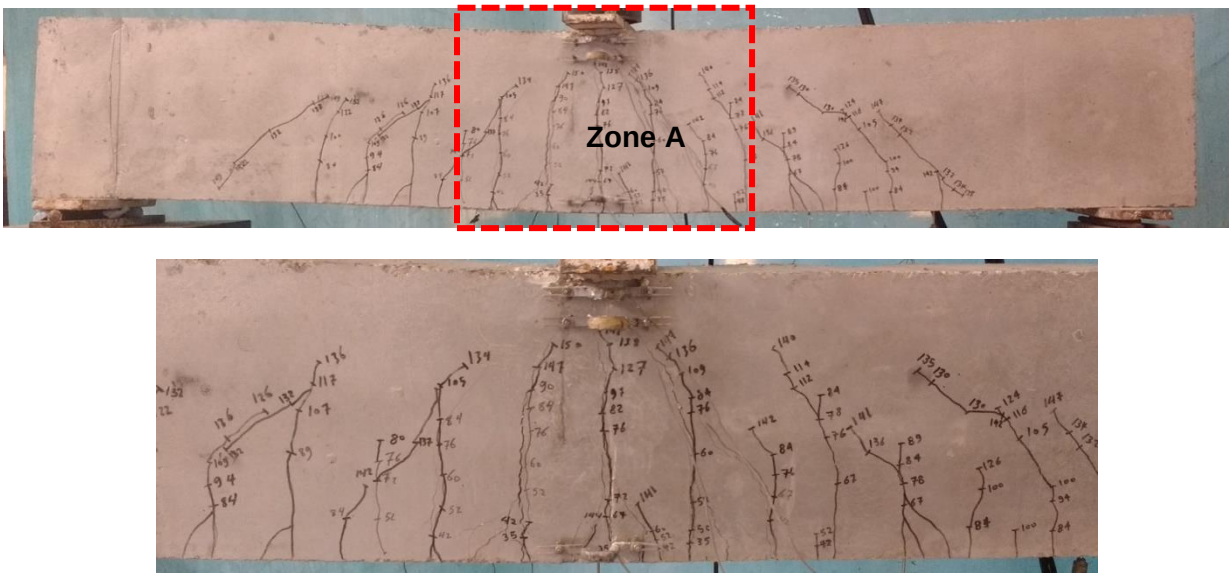

Fig.22. Cracks mapping on the longitudinal sections for solid beam.

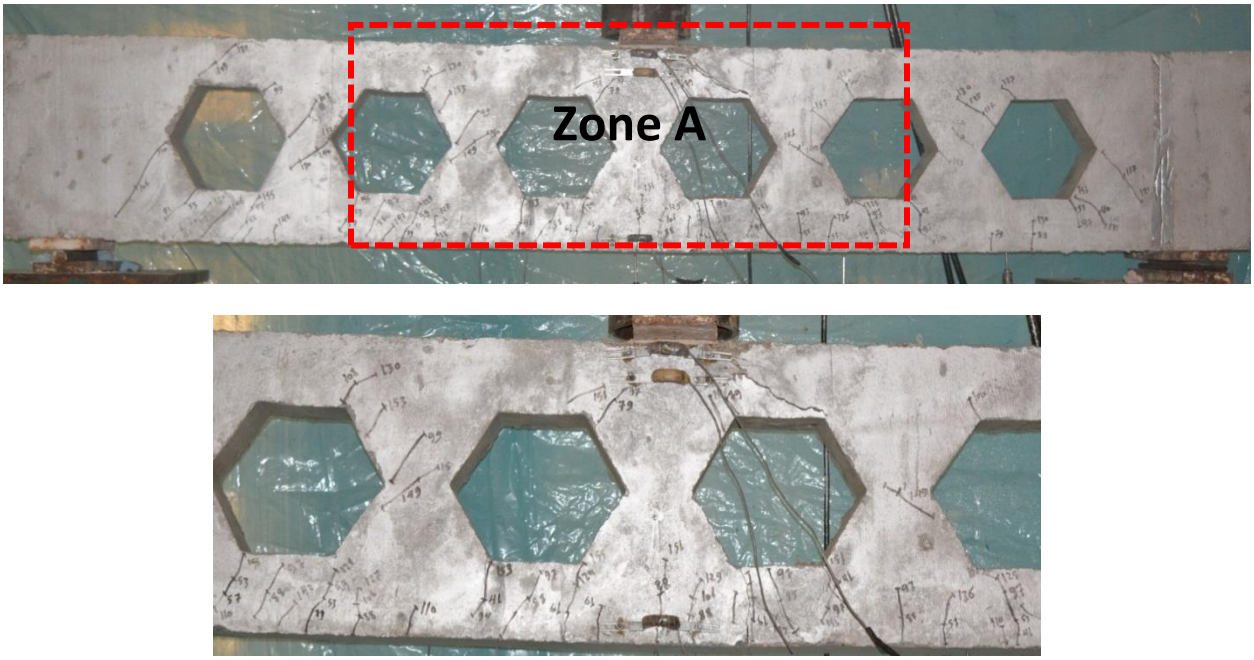

Fig.23. Cracks mapping on the longitudinal sections for castellated beam

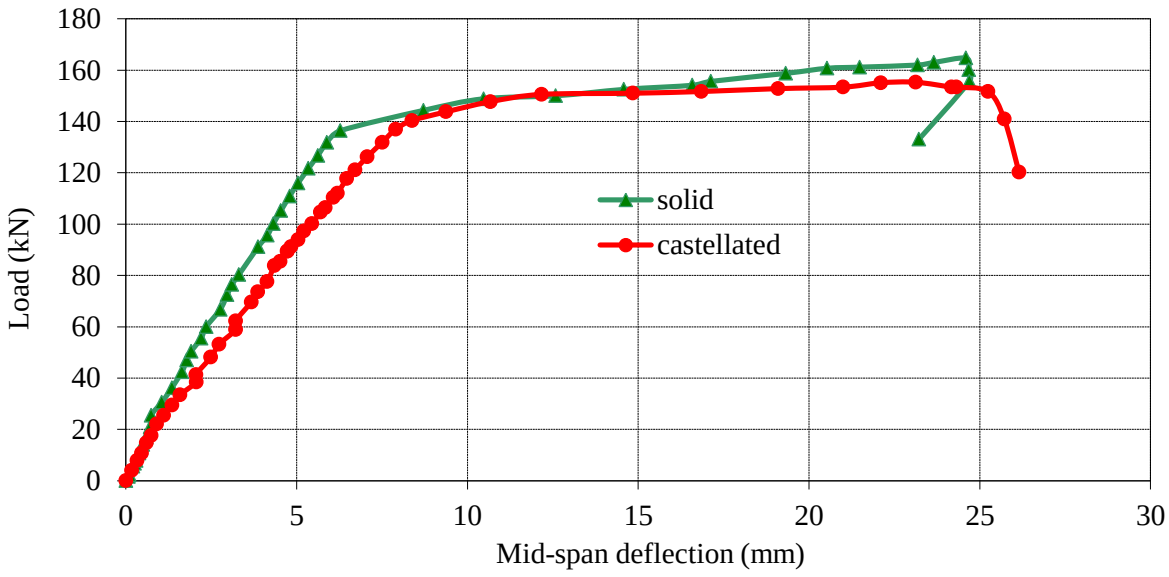

Fig.24. Load-deflection relationship for castellated beam versus that of the solid beam.

CONCLUSION

Based on the results of the numerical simulation and the experimental work results, the following conclusions could be highlighted:

1- Increasing the reinforcement ratio of the main tensile steel affects proportionally on the ultimate capacity of beam. However, the ductility was shown to be inversely proportionate with the amount of main steel.

2- The configuration of the reinforcing steel around the castellation has significant effect on both ultimate capacity and ductility of perforated beams.
3- For solid beam, the ultimate capacity increases with increase the amount of the main tensile steel. On contrary, the developed ductility decreases with increase the amount of the main tensile steel.
4- Increasing the amount of side bars above and below the castellation in castellated beam has slight effect on both ultimate capacity and ductility.
5- Providing castellation affects the initial flexural crack and first shear crack due to the reduction on the concrete section.
6- For beams having castellated perforation of 195 mm diameter (D/t = 0.48), the perforation showed slight decrease in the ultimate capacity by about 5.3 % compared to that of the solid beam. On the other hand, the exhibited ductility was reduced by about 27.8 % compared to that of the solid beam.

.REFERENCES

1- Daniel, J.J., Revathy, J., (2014) "Experimental Investigation on flextural strength of Beams with Opening", Int J Res Manage Tech (IJRMT), Vol. 4, No.2, pp 141-143.
2- Prentzas, E.G., (1968), "Behavior and reinforcement of concrete beams with large rectangular apertures", PhD Thesis, University of Sheffield, UK; p. 230.
3- Al-Sheikh, S.A., (2014), "Flexural behavior of RC beams with opening", Concr Research letters, pp. 812-824.
4- Mansur, M.A., Tan, K.H., Lee, S. L., (1984), "Collapse loads of RC beams with large openings", ASCE J Struct Eng., Vol. 110, No.11, pp 2602-2610.
5- Hasnat, A, Akhtaruzzaman, A.A., (1987), "Beams with small rectangular opening under torsion, bending and shear", ASCE J Struct Eng., Vol. 113, No.10, pp 2253-2270.
6- Somes, N.F., Corley, W.G., (1974), "Circular openings in webs of continuous beams. Shear in Reinforced Concrete", Special Publication SP-42. Detroit: American Concrete Institute, pp.359-398.
7- Mansur, M.A., Tan, K.H., (1999), "Concrete beams with openings: analysis and design". Boca Raton, Florida, USA: CRC Press LLC; p. 220.
8- Aykac,B., and Yilmaz ,M.C.,(2011) "Behaviour and strength of RC beams with regular triangular or circular web openings", Journal of the Faculty of Engineering and Architecture of Gazi University, Vol. 26, No.3, pp 711-718.
9- Saksena, N.H.,patel, P.G., (2013) "Experimental study of reinforced concrete beam with web openings", International Journal of Advanced Engineering Research and Studies, Vol. 2, No.3, pp 66-68.
10- Aykac, B., Kalkan, I., Aykac, S., Egriboz, Y.M., (2013) "Flexural behavior of RC beams with regular square or circular web openings", Engineering Structures, Vol. 56, pp 2165-2174.
11- ABAQUS, ABAQUS Theory manual, version 6.12, Hibbitt, Carlsson and Sorenson, Inc., Pawtucket, RI, USA, 2012.
12- Egyptian code for design and construction of reinforced concrete structures (ECP 203-2017); 2017.
13- Hillerborg, M. M, and P. P.E, (1976) "Analysis of Crack Formation and Crack Growth in Concrete by Means of Fracture Mechanics and Finite Elements", Journal of Cement and Concrete Research, Vol. 6, No. 6, pp. 73-87.
14- Park H, Paulay T. Reinforced concrete structures. New York: John Wiley and Sons; 1975.
15- Atta,A.M., Khalil,A., (2015) "Strengthening of RC beams with opening in shear zone using external prestressing technique", Magazine of Concrete Research, Vol. 67, No. 3, pp. 133-144.
16- Samar Gohar, Hamdy M. Afefy, Nesreen M. Kassem and Salah El-Din F. Taher, (2017) "Flexural performance of self-compacted perforated concrete beams under repeated loading" Engineering Structures, Vol. 143C, July, pp. 441-454.